nature genetics

Pyrexia is a new thermal transient receptor potential channel endowing tolerance to high temperatures in *Drosophila melanogaster*

Youngseok Lee[1,4], Yong Lee[2,4], Jaejung Lee[1], Sunhoe Bang[1], Seogang Hyun[1], Jongkyun Kang[1], Sung-Tae Hong[1], Eunkyung Bae[3], Bong-Kiun Kaang[2] & Jaeseob Kim[1]

Several transient receptor potential channels were recently found to be activated by temperature stimuli *in vitro*[1–14]. Their physiological and behavioral roles are largely unknown. From a temperature-preference behavior screen of 27,000 *Drosophila melanogaster* P-insertion mutants, we isolated a gene, named *pyrexia* (*pyx*), encoding a new transient receptor potential channel. Pyx was opened by temperatures above 40 °C in *Xenopus laevis* oocytes and HEK293T cells. It was ubiquitously expressed along the dendrites of a subset of peripheral nervous system neurons and was more permeable to K^+ than to Na^+. Although some *pyx* alleles resulted in abnormal temperature preferences, *pyx* null flies did not have significantly different temperature preferences than wild-type flies. But 60% of *pyx* null flies were paralyzed within 3 min of exposure to 40 °C, whereas only 9% of wild-type flies were paralyzed by the same stimulus. From these findings, we propose that the primary *in vivo* role of Pyx is to protect flies from high-temperature stress.

All animals have mechanisms to sense the temperature of their surroundings, including reception of temperature stimuli in sensory neurons and processing of the temperature-activated neural signals in the brain. To identify molecules involved in these processes, we carried out a large-scale behavioral genetic screen of more than 27,000 EP-insertional mutant *D. melanogaster* lines (**Supplementary Methods** online). To measure temperature preferences, we constructed an apparatus (**Fig. 1a**), similar to one previously described[15], containing 19 electronic thermal sensors (sensor accuracy of ±0.1 °C) embedded along a 42-cm-long aluminum block that generates a temperature gradient from 14 °C to 44 °C across its length (**Supplementary Fig. 1** online). Wild-type flies placed on this apparatus migrated to their preferred temperature of 25 °C within 20 min in darkness[15] (**Fig. 1b**).

From the screen using this apparatus, we found that pyx^1 and pyx^2 flies have P-element insertions 338 bp and 538 bp, respectively, upstream from the first translation start site of the gene *CG17142* encoding a new transient receptor potential (TRP) channel (**Fig. 1c**; cytological location 61B2). We confirmed the gene structure by sequencing cDNAs obtained by RT-PCR from mRNA from heads of w^{1118} flies. *CG17142* encodes two proteins, Pyx-PA and Pyx-PB, resulting from alternative transcription (**Fig. 1c**). These two Pyx proteins show strong sequence homologies to two previously known thermo-TRP proteins, Painless and dANKTM1 (**Fig. 1d**).

The preferred mean temperatures (PMTs) of pyx^1 and pyx^2 flies were 26.8 °C and 27.5 °C, respectively, compared with 25.3 °C for wild-type flies (**Fig. 2a** and **Table 1**). pyx^1 and pyx^2 flies had no visible morphological or locomotive defects. ANOVA analyses showed that these two *pyx* mutants did prefer different temperatures than did wild-type flies (**Table 1**). In contrast, the PMT of pyx^{R51} flies, revertants of pyx^2 generated by precise P-element excision, was indistinguishable from that of wild-type flies (**Fig. 2b**). RT-PCR analyses showed that expression of Pyx-PA was elevated and expression of Pyx-PB was reduced in pyx^1 and pyx^2 mutants (**Fig. 2c**). These results suggest that the Pyx channel mediates temperature reception.

To investigate this possibility further, we generated two deletion alleles (pyx^{Df4} and pyx^{Df9}) by imprecise P-element excision and one null allele (pyx^3) by P-element local hopping (**Fig. 1c**). pyx^{Df4} expresses only the Pyx-PA transcript; pyx^{Df9} expresses only the Pyx-PB transcript; and pyx^3 does not express either transcript (**Fig. 2d** and **Supplementary Note** online). Behavioral analyses of these mutants showed that pyx^3 ($P = 0.1332$ by ANOVA) and pyx^{Df4} ($P = 0.0659$ by ANOVA) flies had similar temperature preferences to that of wild-type flies (**Fig. 2e**,**f** and **Table 1**). pyx^{Df9} flies had a different temperature preference ($P = 0.0022$ by ANOVA) from that of wild-type flies, although their PMT (25.3 °C) was the same as that of wild-type flies, whereas the PMTs of pyx^3 (24.5 °C) and pyx^{Df4} (24.8 °C) flies were lower than that of wild-type flies (**Table 1**).

To identify behavioral deficits of pyx^3 null flies, we placed them on aluminum blocks of fixed temperature (*i.e.*, no gradient) and determined the fraction of flies paralyzed over a certain period of time. This assay is similar to that used in studies of genetic variation for thermal

[1]Department of Biological Sciences, Korea Advanced Institute of Science & Technology, 373-1 Guseong-Dong, Yuseong-Gu, Daejeon 305-701, Korea. [2]Division of Biological Sciences, Seoul National University, San 56-1 Sillim-Dong, Gwanak-Gu, Seoul 151-742, Korea. [3]GenExel, Inc., KAIST, 373-1 Guseong-Dong, Yuseong-Gu, Daejeon 305-701, Korea. [4]These authors contributed equally to this work. Correspondence should be addressed to J. Kim (kjaeseob@kaist.ac.kr).

Published online 30 January 2005; doi:10.1038/ng1513

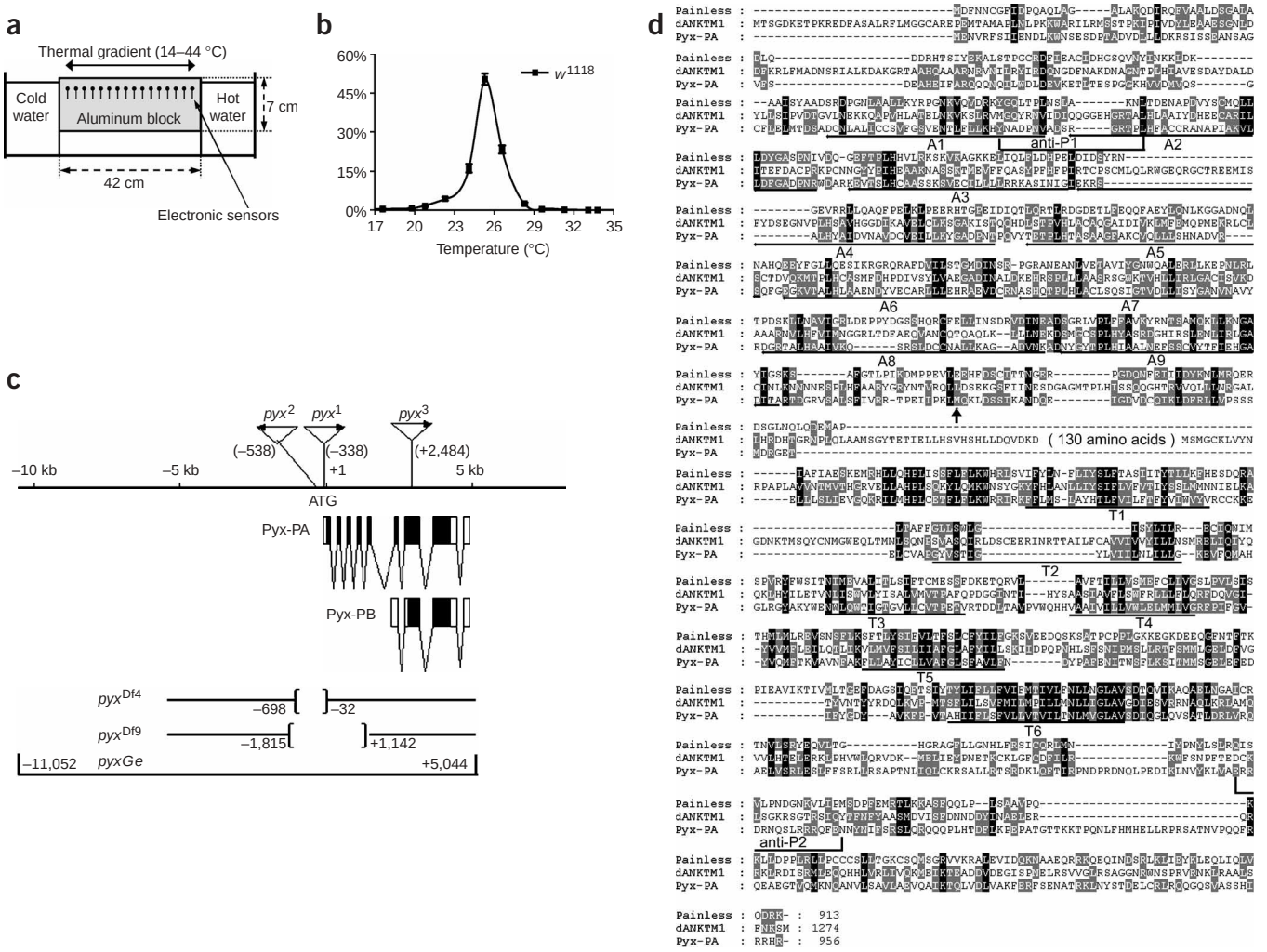

Figure 1 Structure and alleles of *pyx*. (**a**) Diagram of thermal gradient apparatus to assay temperature preference of adult *Drosophila*. The fixture provides a stable temperature gradient ranging from 14 °C to 44 °C along the 42-cm aluminum block (42 cm long × 24 cm wide × 7 cm high) that has electronic thermal sensors embedded every 3 cm. (**b**) Wild-type flies show temperature preference around 25 °C. The *y* axis shows the percentage of flies that populated each temperature range. (**c**) Genomic organization of *pyx* locus and its mutated alleles. Two alternate transcripts, Pyx-PA and Pyx-PB, are shown, with open boxes for noncoding exons and filled boxes for coding exons. The positions of P-element insertions, deletion boundaries and rescue genomic fragment boundaries relative to the translation start site of Pyx-PA are indicated (in bp) for three P-insertion alleles (pyx^1, pyx^2, pyx^3) and two deletion alleles (pyx^{Df4} and pyx^{Df9}). (**d**) Amino acid sequence alignment of Pyx with two *D. melanogaster* TRP proteins involved in temperature sensing. A1–A9, ankyrin repeats; T1–T6, transmembrane domains; anti-P1 and anti-P2, two regions of amino acid sequence used to generate antibodies. The upward arrow indicates the translation start site of Pyx-PB.

resistance in wild-type flies[16]. No *pyx* mutant flies or wild-type flies were paralyzed in 5 min at 37 °C (data not shown). But more than 60% of pyx^3 null flies were paralyzed within 3 min at 40 °C, whereas only 9% of w^{1118} wild-type control flies were paralyzed under these conditions (**Fig. 2h**). pyx^{Df4} and pyx^{Df9} flies were also paralyzed faster than wild-type flies at 40 °C (**Fig. 2h**). The faster paralysis and lower PMT of pyx^3 flies were rescued to values observed in wild-type flies by transformation of the 16-kb genomic DNA fragment spanning the *pyx* locus (**Figs. 1c** and **2g**,**h**). These data suggest that the primary *in vivo* role of Pyx is to protect organisms from high-temperature stress or to endow tolerance to high temperatures.

pyx^1 and pyx^2 flies also had faster paralysis than wild-type flies (**Fig. 2h**). These alleles express elevated levels of Pyx-PA and reduced levels of Pyx-PB, which could result from interferences of enhancers by P-element insertion in the promoter. Hence, proper ratios of Pyx-PA–Pyx-PB heteromers and Pyx-PA or Pyx-PB homomers may not be present in the thermal stress-responsive neurons, resulting in faster paralysis.

Because *pyx* mutants had abnormal response to temperature, we hypothesized that the Pyx channels might be activated by temperature stimuli. To test this possibility, we expressed *pyx* mutants in *X. laevis* oocytes and measured membrane current while gradually increasing the bath temperature from 18 °C to 42 °C (**Fig. 3a–d**). With increasing temperature, oocytes expressing Pyx-PA and oocytes expressing Pyx-PB showed current responses of 3.15 ± 0.32 μA ($n = 20$) and 2.10 ± 0.18 μA ($n = 16$), respectively (**Fig. 3c**,**d**). Such current responses are comparable to those of oocytes expressing vanilloid receptor VR1 (**Fig. 3b**)[10]. Increased current responses of Pyx-PA

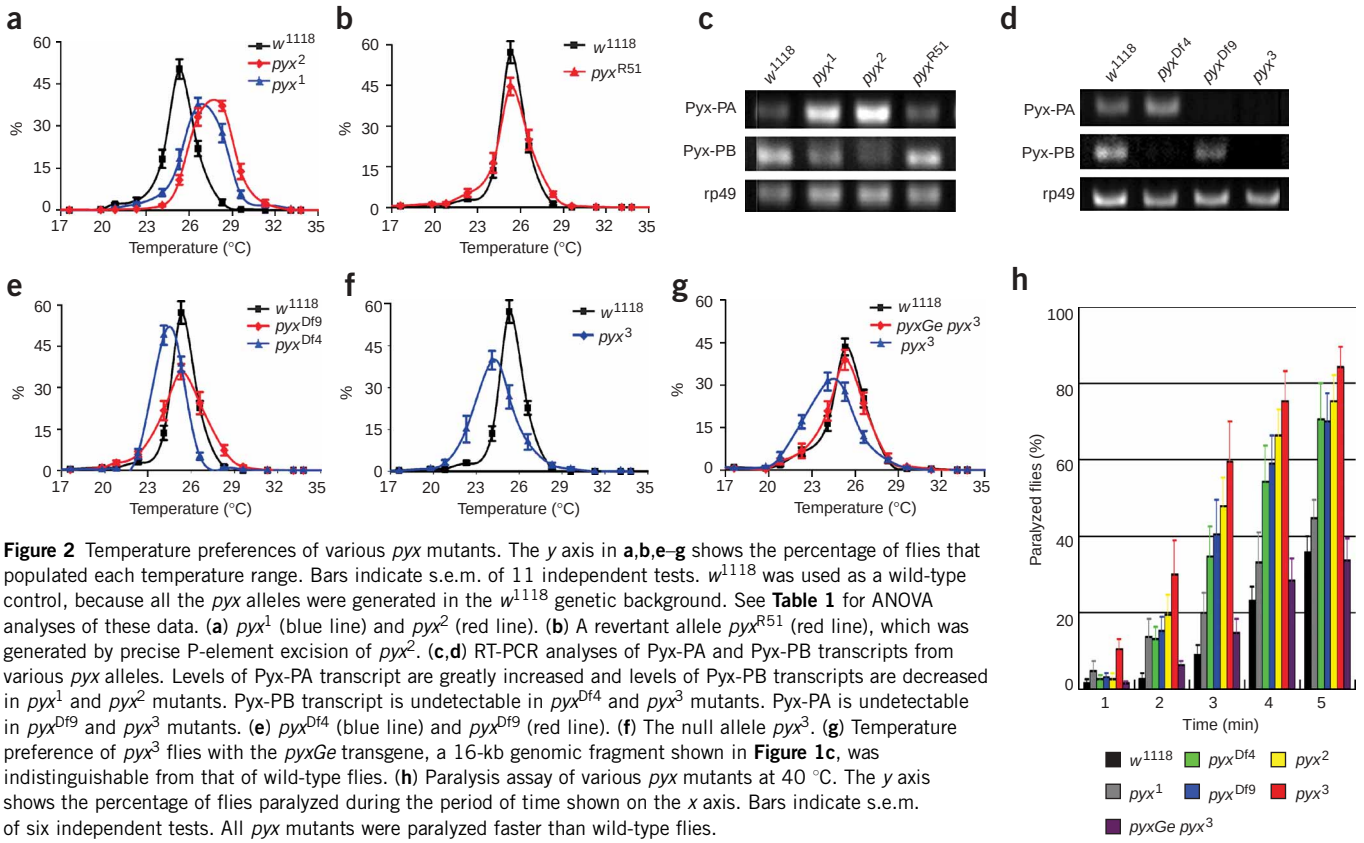

Figure 2 Temperature preferences of various *pyx* mutants. The *y* axis in **a**,**b**,**e**–**g** shows the percentage of flies that populated each temperature range. Bars indicate s.e.m. of 11 independent tests. w^{1118} was used as a wild-type control, because all the *pyx* alleles were generated in the w^{1118} genetic background. See **Table 1** for ANOVA analyses of these data. (**a**) pyx^1 (blue line) and pyx^2 (red line). (**b**) A revertant allele pyx^{R51} (red line), which was generated by precise P-element excision of pyx^2. (**c**,**d**) RT-PCR analyses of Pyx-PA and Pyx-PB transcripts from various *pyx* alleles. Levels of Pyx-PA transcript are greatly increased and levels of Pyx-PB transcripts are decreased in pyx^1 and pyx^2 mutants. Pyx-PB transcript is undetectable in pyx^{Df4} and pyx^3 mutants. Pyx-PA is undetectable in pyx^{Df9} and pyx^3 mutants. (**e**) pyx^{Df4} (blue line) and pyx^{Df9} (red line). (**f**) The null allele pyx^3. (**g**) Temperature preference of pyx^3 flies with the *pyxGe* transgene, a 16-kb genomic fragment shown in **Figure 1c**, was indistinguishable from that of wild-type flies. (**h**) Paralysis assay of various *pyx* mutants at 40 °C. The *y* axis shows the percentage of flies paralyzed during the period of time shown on the *x* axis. Bars indicate s.e.m. of six independent tests. All *pyx* mutants were paralyzed faster than wild-type flies.

and Pyx-PB were not detected when the bath temperature was lower than 35 °C.

To examine further the temperature-dependent activation of the Pyx channels, we expressed *pyx* mutants in HEK293T cells and examined the thermal responses of these cells at –60 mV holding potential while gradually increasing the bath temperature from 22 °C. Consistent with our observations in *X. laevis* oocytes, HEK293T cells expressing Pyx-PA, Pyx-PB or both showed inward currents of 73.2 ± 3.7 pA, 51.3 ± 1.5 pA and 30.5 ± 2.7 pA, respectively, at the temperature stimulus of 40 °C ($n = 5$; **Fig. 3e–g**).

To measure the threshold temperatures more precisely, we carried out voltage-clamp analysis of HEK293T cells expressing Pyx proteins from –100 mV to 100 mV in whole-cell configuration (**Fig. 3h–j**). Cells expressing Pyx-PA had no measurable current at 37.5 °C or lower, but the channel opened rapidly at 40 °C, giving a current of 125.65 ± 4.32 pA ($n = 7$) at 100 mV (**Fig. 3h**). On the other hand,

Table 1 Statistical analyses of variance for the temperature preferences of various *pyx* mutants

			Comparing within replicates				Comparing with wild-type control			
Genotype	Number of flies tested	PMT (°C)	d.f.	Type III SS	F value	*P* value	d.f.	Type III SS	F value	*P* value
w^{1118}	549	25.3	10	0.1251	0.32	0.973				
pyx^1	1,052	26.8	10	0.0625	0.26	0.987	1	0.0161	7.23	**0.0141**
pyx^2	1,196	27.5	10	0.1334	0.53	0.863	1	0.0448	12.24	**0.0023**
w^{1118}	811	25.3	10	0.1483	0.28	0.983				
pyx^{R51}	934	25.3	10	0.1095	0.36	0.961	1	0.0018	3.72	0.0682
pyx^{Df4}	900	24.8	10	0.1562	0.3	0.977	1	0.0035	3.78	0.0659
pyx^{Df9}	998	25.3	10	0.0425	0.19	0.997	1	0.0059	12.34	**0.0022**
pyx^3	815	24.5	10	0.1051	0.36	0.96	1	0.0019	2.45	0.1332
w^{1118}	1,140	25.2	10	0.0447	0.16	0.998				
pyx^3	674	24.3	10	0.0722	0.41	0.938	1	0.0004	0.4	0.5323
pyxGe pyx^3	658	25.2	10	0.0603	0.22	0.993	1	0.0004	1.1	0.3069

ANOVA tests were done with SAS GLM. Sensitivity to environmental effects within each genotype was evaluated by examining replicate structures with the model Y = overall mean + replicate + error. To compare mutant and wild-type flies, the model Y = overall mean + genotype + temperature + replicate (genotype) + error was used. This test showed that pyx^1, pyx^2 and pyx^{Df9} flies had temperature preferences that were statistically different from that of wild-type flies (*P* values in bold). Experiments were done 11 times for each genotype. d.f., degrees of freedom.

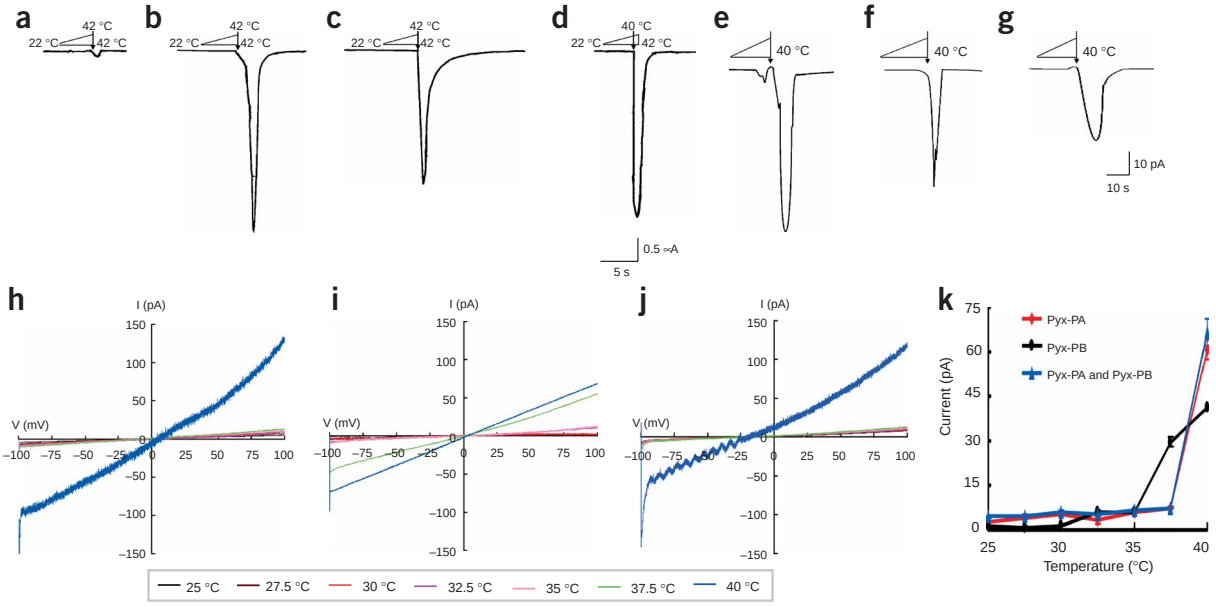

Figure 3 Responses to thermal stimuli in *X. laevis* oocytes and HEK293T cells expressing *D. melanogaster* Pyx. (**a**–**d**) Representative current traces recorded in *X. laevis* control oocytes (**a**; 0.23 ± 0.12 μA, $n = 13$), oocytes expressing vanilloid receptor VR1 (**b**; 3.57 ± 0.76 μA, $n = 6$), oocytes expressing Pyx-PB (**c**; 2.10 ± 0.18 μA, $n = 16$) and oocytes expressing Pyx-PA (**d**; 3.15 ± 0.32 μA, $n = 20$). (**e**–**g**) Inward currents in Pyx-expressing HEK293T cells were evoked at –60 mV holding potential by increasing the temperature stimulus from 25 °C to 40 °C ($n = 5$). (**e**) Pyx-PA (73.2 ± 3.7 pA at 40 °C). (**f**) Pyx-PB (51.3 ± 1.5 pA at 40 °C). (**g**) Pyx-PA and Pyx-PB (30.5 ± 2.7 pA at 40 °C). (**h**–**j**) Temperature sensitivities of Pyx-PA and Pyx-PB in HEK293T cells. Traces are the mean values of five or seven independent experiments. (**h**) Pyx-PA was activated at 40 °C but silent at 37.5 °C or lower. (**i**) Pyx-PB was opened at 37.5 °C or higher but silent at 35 °C or lower. (**j**) Cells expressing Pyx-PA and Pyx-PB together were silent at 37.5 °C or lower but markedly activated at 40 °C with a sudden current increase. The reversal potential was shifted to approximately –16 mV in these cells. (**k**) A temperature-response current curve of Pyx channels expressed in HEK293T cells at 60 mV.

cells expressing Pyx-PB had a current at 37.5 °C (53.95 ± 1.25 pA at 100 mV, $n = 5$), but not at 35 °C or lower (**Fig. 3i**), and the current increased slightly at 40 °C (**Fig. 3i**).

TRP channels tend to form tetramers. Because immunostaining with P1 and P2 antibodies, which recognize Pyx-PA and Pyx PA plus Pyx-PB, respectively, gave identical patterns (**Fig. 1d**, and data not shown), Pyx-PA and Pyx-PB probably form heteromers *in vivo*. Therefore, we examined the current responses in HEK293T cells expressing both Pyx-PA and Pyx-PB (1:1 ratio). These cells had no measurable current at 37.5 °C or lower (**Fig. 3j**) but showed a marked current increase (121.15 ± 0.3 pA at 100 mV, $n = 7$; **Fig. 3j**) at 40 °C.

The reversal potential was shifted to –16 ± 3.5 mV in cells expressing both Pyx-PA and Pyx-PB (**Fig. 3j**). To explore this finding further, we measured relative ion permeability of Pyx channels (**Table 2** and **Supplementary Fig. 2** online). Consistent with the shifted reversal potential, the heteromeric channels were 80% and 54% more permeable to K^+ and Cs^+, respectively, than to Na^+ (**Table 2**). In contrast, Pyx-PA and Pyx-PB homomeric channels did not show significant selective ion permeability (**Table 2**).

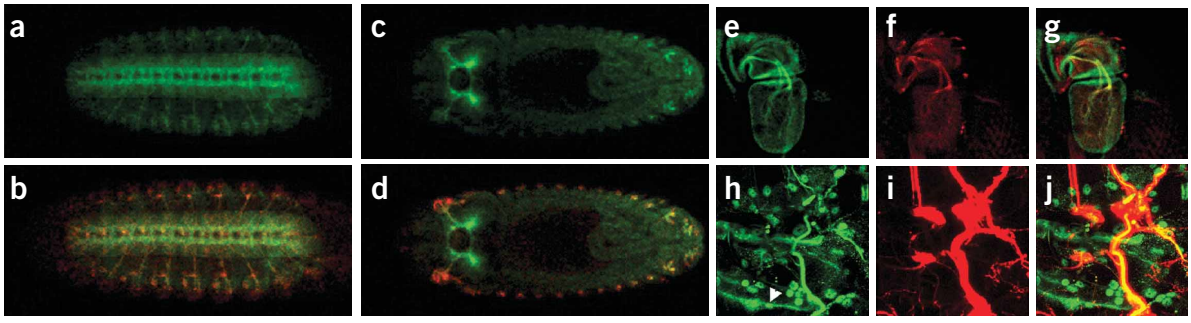

Figure 4 Confocal microscopic images of Pyx-expressing neurons. (**a**–**g**) Immunostains of w^{1118} flies with Pyx P1 antibody (green) and mAb22C10 (red). mAb22C10 marks neuronal cells in *D. melanogaster*. (**a**–**d**) Embryos at stage 16. Ventral view (**a**,**b**) and dorsal view (**c**,**d**). (**b**,**d**) Merged image of **a** and **c** with mAb22C10 stain. (**e**–**g**) Pupal antenna. (**g**) Merged image of **e** and **f**. (**h**–**j**) Immunostaining analyses to compare Pyx-expressing neurons with multidendritic neurons. The membrane-targeted GFP (mCD8GFP) driven by md-GAL4, which marks multidendritic neurons in larval epidermis, is shown in red, and the Pyx proteins visualized by Pyx antibody are shown in green. (**j**) Merged image of **h** and **i**. Note the strong ubiquitous expression of Pyx along the dendrites. Some Pyx-expressing neurons are not multidendritic neurons (arrowhead in **h**).

Table 2 The relative ion permeability of Pyx channels measured in HEK293T cells

Relative permeability	Pyx-PA	Pyx-PB	Pyx-PA and Pyx-PB
p_K/p_{Na}	1.009	1.025	1.798
p_{Cs}/p_{Na}	1.235	1.197	1.544
p_{Ca}/p_{Na}	0.605	0.617	0.663

The relative permeability of each ion was calculated as follows: $p_x/p_{Na} = \exp(\Delta V_{rev}F/RT)$ for monovalent ion and $p_x/p_{Na} = [Na^+]_i\exp(\Delta V_{rev}F/RT)(1+\exp(\Delta V_{rev}F/RT))/4[X^{2+}]_o$ for divalent ion, where V_{rev} is reversal potential, F is Faraday's constant, R is the universal gas constant and T is absolute temperature[10].

Channels were less permeable to the divalent cation Ca^{2+} than to Na^+ (**Table 2**).

Pyx channel activities were not blocked by the TRP channel blocker ruthenium red or by treatment with 5 mM EGTA in either *X. laevis* oocytes or HEK293T cells. The latter result implies that opening of Pyx at 40 °C is not gated by Ca^{2+} ions liberated nonspecifically from intracellular Ca^{2+} stores, but rather is gated specifically by high-temperature stimuli. This interpretation is further supported by observations that the Q_{10} values of Pyx channels in the range of 30–40 °C were 18.145 for Pyx-PA, 15.329 for Pyx-PB and 18.064 for the Pyx-Pa–Pyx-PB heteromers. These Q_{10} values are different from those of non-thermo-TRP channels, which have Q_{10} values of ~1.5. Therefore, we conclude that Pyx is gated by temperature stimuli.

To understand better the mechanisms of Pyx function, we examined the location of Pyx expression *in vivo*. Pyx was expressed in various peripheral nerves and the central nerves in embryos (**Fig. 4a–d**). In adults, it was expressed in sensory neurons lying beneath the bristles around eyes, neurons innervating the bristles on the back of thorax and neurons in maxillary palps, proboscis (data not shown) and antennae (**Fig. 4e–g**). Accordingly, Pyx-expressing neurons were widely distributed throughout the fly body and might enable efficient responses to high temperatures in nature.

Multidendritic neurons mediate temperature sensing[12,17]. We examined whether Pyx was also expressed in these neurons. Analysis of UAS-mCD8-GFP flies with multidendritic neuronal GAL4 (ref. 18) stained with Pyx antibody showed that Pyx was expressed in multidendritic neurons as well as nonmultidendritic neurons in larval epidermis (**Fig. 4h–j**).

Pyx is not localized at the tip or in local structures of the neuronal axon but exists throughout the neurites (**Fig. 4**), unlike other channels that sense external stimuli. The ubiquitous distribution of Pyx proteins throughout neurites, fast paralysis of *pyx* null flies (**Fig. 2h**), opening of the Pyx channel by high temperature (**Fig. 3**) and selectivity of Pyx-PA–Pyx-PB heteromers for K^+ ion (**Table 2**) are consistent with Pyx acting to protect neurons from inappropriate firing during high-temperature stress. Because flies have large ratios of volume to weight, like other small insects, which cause fast heat exchange between body and environment, their body temperatures can rise by 10 °C on exposure to unfiltered sunlight for only 10 s (ref. 19). Therefore, Pyx-mediated thermal stress protection might have evolved to allow flies to survive in natural environments.

METHODS

***D. melanogaster* strains and genomic rescue of *pyx*^{3} mutants.** We obtained EP mutant flies from GenExel, Inc. Strain GAL4109(2)80(md-GAL4) combined with UAS-mCD8GFP was provided by Y.N. Jan (University of California at San Francisco). We carried out imprecise excision and local hopping using standard techniques and a *pyx*^{2} mutant with a TMSΔ2-3 chromosome as the P-transposase source. We generated the genomic rescue construct of *pyxGe* as follows. We isolated the 8,486-bp *Sph*I-*Stu*I fragment from BACR11J11 and added an *Xba*I site to the end of the *Stu*I site by subcloning into pBluescript (Stratagene). We cloned this fragment and the 7,612-bp *Kpn*I-*Sph*I fragment isolated from BACR11J11 into the *Kpn*I-*Xba*I site of CaSper vector. We produced the transgenic lines in a *w*^{1118} background using standard techniques.

Temperature preference behavioral assay. We suspended a glass plate coated with fly repellent (quinine sulfate) 5 mm over the aluminum block (**Fig. 1a** and **Supplementary Fig. 1** online). We placed ~50–100 adult flies between the aluminum block and the glass plate and allowed them to migrate in darkness for 20 min. We took photographs with a digital camera.

cDNA cloning and Pyx expression constructs. We generated the cDNA pool by RT-PCR of mRNA prepared from the heads of *w*^{1118} flies. We amplified the predicted transcripts using *pfu* polymerase (Bioneer). We subcloned Pyx-PA and Pyx-PB into pcDNA3 vector for expression in mammalian cells. We cleaved Pyx-PB in pcDNA3 plasmid with *Eco*RI and cloned the resulting 1.6-kb fragment into the *Eco*RI site of the *X. laevis* oocyte expression vector pSDR-ER. We confirmed the orientation of the fragment confirmed by restriction enzyme digestion. We cleaved Pyx-PA sequences in the pcDNA3 plasmid with *Nhe*I and *Xho*I and ligated the resulting 2.9-kb fragment to *Spe*I-*Xho*I–cleaved oocyte expression vector. After linearizing the plasmid with *Xba*I, we prepared cRNAs of both Pyx-PA and Pyx-PB by *in vitro* transcription using the cRNA Megascript Kit (Ambion).

Electrophysiological recording. We prepared *X. laevis* oocytes and carried out cRNA microinjection as described previously[10,20]. We held *X. laevis* oocytes at 18 °C and the membrane potential at –70 mV. After the basal current was stabilized, we raised the temperature at the rate of 1 °C s^{-1} and measured the resulting current. We stored the current values digitally on video cassette tape using Digidata (Instrutech) for later analysis. We recorded HEK293T cells in whole-cell configuration. We obtained giga-seal by glass electrodes (G120T-4, Warner Instruments) with resistance ranging from 3 to 5 MΩ. The pipette solution contained 140 mM CsCl, 5 mM EGTA and 10 mM HEPES buffer (pH 7.4). The cell capacitance and series resistance were compensated manually. We perfused cells with bath solution (140 mM NaCl, 8 mM KCl, 2 mM $MgCl_2$, 10 mM HEPES buffer and 10 mM glucose (pH 7.4)). We raised the temperature at the rate of 1 °C s^{-1} from 22 °C to 40 °C using a TC-342B single channel heater controller and SH-27B solution in-line heater (Warner Instruments). We held the temperature at room temperature (22 °C) during basal current recording in HEK293T cells. We raised the temperature by 2.5 °C s^{-1} with a temperature controller and with in-line heater units to find the threshold temperature of Pyx channels. To analyze Pyx channel temperature-dependent properties, we raised the temperature by 1 °C s^{-1}. We recorded the currents through Pyx using Axopatch 200B and pClamp6 program (Axon Instruments, Inc.) by ramp voltage clamp from –100 mV to 100 mV to obtain the I – V relationship. We filtered the records at 2 kHz and stored the data digitally. For Q_{10} values, we normalized the currents at each temperature to values at 25 °C and calculated E_a/R as follows: $-E_a/R = 2.303\log_{10}[(I_2/I_1)/((1/T_2) - (1/T_1))]$, where I_2 is the normalized current at higher temperature T_2 (in K), and I_1 is the normalized current at lower temperature T_1. After calculating E_a/R, we obtained Q_{10} values as follows: $Q_{10} = \exp((10\ E_a/R)/(T_1T_2))$. For ion substitution experiments, we recorded HEK293T cells expressing Pyx channels in whole-cell configuration. The pipette solution contained 140 mM NaCl and 10 mM HEPES buffer (pH 7.4). The bath solution contained 140 mM NaCl, 10 mM glucose and 10 mM HEPES buffer (pH 7.4). After whole-cell configuration was achieved, we substituted the bath solution with a solution containing 140 mM KCl, 140 mM CsCl or 110 mM $CaCl_2$ instead of 140 mM NaCl.

Immunohistochemical staining. For fluorescence immunostaining of pupae, we resected the anterior half of the pupal case and fixed it overnight in standard fixative solution. The next day, we removed the rest of the pupal case and the cuticles surrounding the tissues. We carried out antibody staining of these tissues and larval and embryonic tissues using a procedure described previously[21]. We generated peptide antibodies in rabbits against the sequence shown in **Figure 1d**.

Note: Supplementary information is available on the Nature Genetics website.

ACKNOWLEDGMENTS

We thank D. Stafford for help in preparation of this manuscript, J.J. Park for help in statistical analysis and Y. Jan for the GAL4109(2)80(md-GAL4);UAS-mCD8GFP fly stock. This research has been supported by grants from Brain Research Center of the 21st Century Frontier Program, Korea Science and Engineering Foundation, NRL and Biodiscovery program funded by the Ministry of Science and Technology of Korea.

COMPETING INTERESTS STATEMENT

The authors declare that they have no competing financial interests.

Received 5 October; accepted 24 December 2004
Published online at http://www.nature.com/naturegenetics/

1. Story, G.M. *et al.* ANKTM1, a TRP-like channel expressed in nociceptive neurons, is activated by cold temperatures. *Cell* **112**, 819–829 (2003).
2. Peier, A.M. *et al.* A TRP channel that senses cold stimuli and menthol. *Cell* **108**, 705–715 (2002).
3. McKemy, D.D., Neuhausser, W.M. & Julius, D. Identification of a cold receptor reveals a general role for TRP channels in thermosensation. *Nature* **416**, 52–58 (2002).
4. Viswanath, V. *et al.* Opposite thermosensor in fruitfly and mouse. *Nature* **423**, 822–823 (2003).
5. Watanabe, H. *et al.* Heat-evoked activation of TRPV4 channels in a HEK293 cell expression system and in native mouse aorta endothelial cells. *J. Biol. Chem.* **277**, 47044–47051 (2002).
6. Guler, A.D. *et al.* Heat-evoked activation of the ion channel, TRPV4. *J. Neurosci.* **22**, 6408–6814 (2002).
7. Peier, A.M. *et al.* A heat-sensitive TRP channel expressed in keratinocytes. *Science* **296**, 2046–2049 (2002).
8. Smith, G.D. *et al.* TRPV3 is a temperature-sensitive vanilloid receptor-like protein. *Nature* **418**, 186–190 (2002).
9. Xu, H. *et al.* TRPV3 is a calcium-permeable temperature-sensitive cation channel. *Nature* **418**, 181–186 (2002).
10. Caterina, M.J. *et al.* The capsaicin receptor: a heat-activated ion channel in the pain pathway. *Nature* **389**, 816–824 (1997).
11. Caterina, M.J., Rosen, T.A., Tominaga, M., Brake, A.J. & Julius, D. A capsaicin-receptor homologue with a high threshold for noxious heat. *Nature* **398**, 436–441 (1999).
12. Tracey, W.D., Wilson, R.I., Laurent, G. & Benzer, S. *painless, a Drosophila* gene essential for nociception. *Cell* **113**, 261–273 (2003).
13. Caterina, M.J. *et al.* Impaired nociception and pain sensation in mice lacking the capsaicin receptor. *Science* **288**, 306–313 (2000).
14. Davis, J.B. *et al.* Vanilloid receptor-1 is essential for inflammatory thermal hyperalgesia. *Nature* **405**, 183–187 (2000).
15. Sayeed, O. & Benzer, S. Behavioral genetics of thermosensation and hygrosensation in *Drosophila*. *Proc. Natl Acad. Sci. USA* **93**, 6079–6084 (1996).
16. Gilchrist, G.W. & Huey, R.B. The direct response of *Drosophila melanogaster* to selection on knockdown temperature. *Heredity* **83**, 15–29 (1999).
17. Liu, L., Yermolaieva, O., Johnson, W.A., Abboud, F.M. & Welsh, M.J. Identification and function of thermosensory neurons in *Drosophila* larvae. *Nat. Neurosci.* **6**, 267–273 (2003).
18. Gao, F.B., Brenman, J.E., Jan, L.Y. & Jan, Y.N. Genes regulating dendritic outgrowth, branching, and routing in *Drosophila*. *Genes Dev.* **13**, 2549–2561 (1999).
19. Heiinrich, B. *The Hot-Blooded Insects: Strategies and Mechanisms of Thermoregulation* (Harvard University Press, Cambridge, Massachusetts, 1993).
20. Lee, Y. β-Amyloid peptide binding protein does not couple to G protein in heterologous *Xenopus* expression system. *J. Neurosci. Res.* **73**, 255–259 (2003).
21. Kim, J. *et al.* Integration of positional signals and regulation of wing formation and identity by *Drosophila* vestigial gene. *Nature* **382**, 133–138 (1996).